A reproductive arrest program triggered by defects in Piwi and germ granules

Short title: Germ granule dysfunction phenocopies Piwi sterility

Authors: Maya Spichal[1,2]†, Bree Heestand[1,2,3]†, Katherine Kretovich Billmyre[1,2]†, Stephen Frenk[1,2]† and Shawn Ahmed[1,2,3*]

Affiliations:

[1]Department of Genetics, University of North Carolina, Chapel Hill, NC, USA

[2]Department of Biology, University of North Carolina, Chapel Hill, NC, USA

[3]Lineberger Comprehensive Cancer Center, University of North Carolina, Chapel Hill, NC, USA

†These authors contributed equally to this manuscript

*Corresponding author: shawn@med.unc.edu

Abstract:

In several species, Piwi/piRNA genome silencing defects lead to immediate sterility accompanied by heterochromatin dysfunction and transposon-induced genomic instability, which may cause Piwi mutant sterility. In *C. elegans,* Piwi pathway mutants transmit a heritable stress through germ cells that induces sterility after growth for several generations. We found that sterile Piwi pathway mutant germ cells displayed inconsistent increases in DNA damage but consistently altered perinuclear germ granules that are known to promote fertility. Germ granule dysfunction did not elicit transposon expression but was sufficient to induce multiple phenotypes found in sterile Piwi silencing mutants, including germline atrophy and regrowth. Furthermore, loss of the germ granule component PGL-1 accelerated sterility in response to deficiency for *prg-1*/Piwi. Restoration of germ granule function to sterile *pgl-1* mutants restored their fertility. Together, our results suggest that germ granule defects may promote an adult reproductive arrest phenotype that is responsible for Piwi/piRNA mutant sterility.

Keywords: Germ granules, reproductive arrest, small RNAs, heterochromatin, germ cell immortality, heritable stress, Piwi

Introduction:

Germ cells give rise to the mortal somatic tissues while maintaining themselves in a pristine condition that allows them to be propagated for an indefinite number of generations. This capacity for self-renewal is termed “germ cell immortality”, and

46 functions to protect the germline from forms of damage that can result in sterility
47 (Smelick and Ahmed, 2005a). Defects in *Caenorhabditis elegans* (*C. elegans)* genes
48 that promote germline immortality cause a Mortal Germline (Mrt) phenotype, where
49 robust fertility occurs for several generations but then deteriorates and finally culminates
50 in complete sterility. The transgenerational sterility of *mrt* mutants implies that their germ
51 cells may age as they proliferate over the generations such that they accumulate a form
52 of damage that ultimately evokes sterility. Identifying the transgenerational damage that
53 accumulates in *mrt* mutant germ cells and the mechanism(s) by which this damage
54 induces sterility are central questions relevant to understanding the basis of germ cell
55 immortality.

56 The initial germline immortality pathway defined in *C. elegans* was promoted by
57 telomerase, a reverse transcriptase that maintains telomere length and stability by
58 adding *de novo* telomere repeats to chromosome termini. *C. elegans* mutants that are
59 defective for telomerase-mediated telomere repeat addition display progressive
60 telomere erosion. In later generations, some telomeres become critically short and fuse
61 together, leading to accumulation of end-to-end chromosome fusions (Lowden et al.,
62 2008; Meier et al., 2006). The precise cause of telomerase mutant sterility remains
63 uncertain (Karlseder et al., 1999; Nakamura et al., 1998; Sharpless and DePinho, 2007;
64 Shay and Wright, 2005), but might be the creation of circular chromosomes that are
65 toxic in meiosis (Nakamura et al., 1998).

66 Most human somatic cells can proliferate *in vitro* for a limited number of divisions
67 before they enter a state of irreversible cell cycle arrest termed senescence (Sharpless
68 and DePinho, 2007; Shay and Wright, 2005). Senescent cells are large and flattened in

comparison to proliferating cells, they express senescence-associated beta-galactosidase and the tumor suppressor protein p16, and they secrete growth factors such as IL6 and IL8 cytokines that act in a cell-non-autonomous manner to promote aging (Tchkonia et al., 2013).The limited proliferative capacity of primary human somatic cells is called ‘replicative aging’. Lack of telomerase is thought to cause replicative aging in humans, because 1) most primary human somatic cells lack detectable telomerase activity *in vitro* (Counter et al., 1992; Shay and Wright, 2000), 2) primary human somatic cells experience progressive telomere erosion as they divide (Harley et al., 1990), 3) senescent cells display DNA damage response foci at telomeres that activate p53 to induce senescence (Fagagna et al., 2003; Herbig et al., 2004), and 4) because senescence does not occur if telomerase activity is restored by expression of the telomerase reverse transcriptase TERT, which is typically silenced in human somatic cells (Bodnar et al., 1998). Support for the model that telomere attrition induces senescence in humans was provided by acute knockdown of the telomere capping protein TRF2, which results in deprotection of telomeres that are normal in length, accompanied by DNA damage response foci at telomeres and senescence (Karlseder et al., 1999). Together, the above data support a model that telomere uncapping results in DNA damage response that activates p53 to cause senescence in human somatic cells.

Other forms of stress can accumulate to cause replicative aging of mammalian somatic cells. For example, expression of the p16 protein induces senescence and increases by orders of magnitude in mouse and human tissues with age, even though mouse somatic cells express telomerase (Krishnamurthy et al., 2004, 2006; Sharpless

92 and DePinho, 2007). Forms of stress that accumulate during replicative aging of
93 mammalian cells may be revealed by analysis of *C. elegans mortal germline* mutants,
94 which display transgenerational sterility phenotypes that could reflect 'replicative aging'
95 of germ cells. In this regard, deficiency for Piwi/piRNAs and related small RNA-
96 mediated genome silencing proteins like RSD-6 and HRDE-1 results in
97 transgenerational sterility in the absence of end-to-end chromosome fusions, indicating
98 that telomere uncapping does not cause sterility of Piwi/piRNA genome silencing
99 mutants (Billmyre et al., 2019; Buckley et al., 2012; Sakaguchi et al., 2014; Simon et al.,
100 2014a).

101 P-M Hybrid Dysgenesis was discovered in the 1970's as a temperature-sensitive
102 *Drosophila* sterility defect that was linked to high levels of transposition (Kelleher, 2016;
103 Kidwell et al., 1977), which occurs in response to lack of piRNA-mediated genome
104 silencing of specific transposable elements (Brennecke et al., 2008a). Piwi is a
105 conserved Argonaute protein that interacts with thousands of piRNAs in germ cells to
106 repress expression of transposons and foreign nucleic acids that represent parasitic
107 threats to the integrity of the genome (Aravin et al., 2007; Luteijn and Ketting, 2013;
108 Siomi et al., 2011). Deficiency for Piwi proteins leads to immediate sterility in
109 *Drosophila*, zebrafish and mouse, which correlates with increased transposon
110 expression and DNA damage in sterile animals (Juliano et al., 2011; Kelleher, 2016;
111 Siomi et al., 2011). Although this implies that transposon-induced genome instability
112 could cause sterility of Piwi mutants, analysis of *Drosophila* strains with variable levels
113 of transposons suggested that transposon-induced genome instability may only explain

114 a minor fraction of P-M hybrid sterility (Srivastav and Kelleher, 2017). Therefore, the
115 cause of sterility in Piwi mutants remains an unsolved problem in experimental biology.
116 Deficiency for the *C. elegans* Piwi ortholog *prg-1* compromises germ cell
117 immortality (Simon et al., 2014b), rather than inducing the immediate sterility phenotype
118 that is observed in Piwi mutants in some other species. The reason for the
119 transgenerational delay in the onset of sterility in *prg-1*/Piwi mutants and in related Piwi
120 pathway mutants of *C. elegans* is not clear, but it is possible that genomic silencing
121 marks that are induced by the Piwi/piRNA pathway are more robustly maintained in
122 germ cells of *C. elegans* if the Piwi silencing system is inactivated. The
123 transgenerational damage that accumulates in *C. elegans* Piwi mutants may therefore
124 correspond to progressive deterioration of Piwi-mediated heterochromatin.
125 Heterochromatin dysfunction in *C. elegans* has been associated with increased
126 levels of transposon and tandem repeat expression, with RNA-DNA hybrid formation,
127 and with transposon-induced DNA damage (McMurchy et al., 2017; Padeken et al.,
128 2019; Zeller et al., 2016). However, very low levels of transposition occur in late-
129 generation *prg-1* mutants, and *C. elegans mutator* mutants, which display high levels of
130 transposition, do not become sterile if grown at low temperatures, suggesting that
131 transposition is unlikley to cause transgenerational sterility of *prg-1*/Piwi mutants (Simon
132 et al., 2014b).
133 Sterile late-generation *C. elegans prg-1*/Piwi mutants display an unusual
134 pleiotropic germ cell degeneration phenotype as L4 larvae mature into 1 day old adults,
135 such that most animals display ‘atrophied’ germlines that contain a small population of
136 mitotic germ cells, whereas some germlines are ‘empty’ and lack germ cells altogether,

137 some germlines are ‘short’ such that they have fewer germ cells than normal but
138 possess both mitotic and meiotic germ cells, and some germlines are sterile but ‘normal’
139 in size such that they are not smaller than germlines of fertile late-generation *prg-1*
140 mutant siblings (Heestand et al., 2018). Similarly, growth of *C. elegans* Piwi pathway
141 mutants *rsd-6*, *nrde-2* and *hrde-1* at the restrictive temperature of 25°C for several
142 generations results in sterile late-generation L4 larvae with germlines that are
143 predominantly normal in size, but these larvae mature into sterile adults that possess
144 germline arms with variable sizes, including small, atrophied and empty (Billmyre et al.,
145 2019; Sakaguchi et al., 2014). The histone 3 lysine 4 demethylase RBR-2 also
146 promotes germ cell immortality at 25°C and may promote genome silencing
147 downstream of small RNAs (Alvares et al., 2014).

148 Atrophied germ lines of sterile *prg-1* mutants can regrow on day 2 of adulthood,
149 and fertility can be restored to a minor fraction of sterile late-generation *prg-1* mutants
150 by altering their food source (Heestand et al., 2018; Simon et al., 2014a). This implies
151 that Piwi mutant sterility is a reversible form of reproductive arrest, also known as Adult
152 Reproductive Diapause or Reproductive Quiescence, which can be induced in response
153 to severe environmental stresses such as starvation (Angelo and Van Gilst, 2009;
154 Padilla and Ladage, 2012; Tatar and Yin, 2001). We therefore proposed that late-
155 generation sterility of *prg-1*/Piwi mutants may occur in response to accumulation of a
156 heritable stress that is transmitted by germ cells (Heestand et al., 2018).

157 Some Argonaute proteins that regulate silencing of the epigenome, like PRG-
158 1/Piwi, are located in germ granules, which are perinuclear structures that interact with
159 nuclear pore complexes and have been previously demonstrated to be necessary for

160 fertility (Fig. 6A) (Updike et al., 2011). *C. elegans* germ granules are termed P granules
161 based on antibodies that label the P blastomere that generates the germ cell lineage
162 (Strome and Wood, 1982). Here we study the late-generation sterility phenotype of Piwi
163 pathway genome silencing mutants and find that it is associated with abnormalities of
164 germ granules. We show that germ granule dysfunction can induce reproductive arrest
165 and that germ granule dysfunction interacts with Piwi deficiency to promote sterility.
166

167 **Results:**

168

169 **Genome instability in Piwi pathway genome silencing mutants**

170 Transgenerational sterility in *C. elegans* telomerase mutants that lack the ability to
171 maintain sequences that cap chromosome ends is caused by high levels of telomere
172 fusions and associated genome damage (Meier et al., 2006). Many *mrt* mutants only
173 become sterile when grown at the non-permissive temperature 25°C (Ahmed and
174 Hodgkin, 2000), some of which are deficient for Piwi pathway-mediated genome
175 silencing (Ashe et al., 2012; Buckley et al., 2012; Burkhart et al., 2011; McMurchy et al.,
176 2017; Sakaguchi et al., 2014; Smelick and Ahmed, 2005b; Spracklin et al., 2017).
177 However, the deficiency for the Piwi Argonaute protein PRG-1 or the nuclear RNA
178 interference (RNAi) proteins NRDE-1 or NRDE-4 results in progressive sterility at any
179 temperature (Batista et al., 2008; Buckley et al., 2012; Burkhart et al., 2011; Das et al.,
180 2008; McMurchy et al., 2017; Simon et al., 2014b). We asked if DNA damage is directly
181 associated with the sterility of Piwi pathway mutants by comparing fertile late-generation
182 Piwi pathway mutants with late generation siblings that were sterile, using both

183 temperature-sensitive Piwi pathway mutants that become sterile at 25°C and non-
184 conditional mutants that become sterile when grown at 20°C.

185 Although DNA damage has been suggested not to contribute significantly to the
186 sterility of *prg-1* mutants (Simon et al., 2014b), DNA damage signaling in sterile *prg-1*
187 mutant animals has not been previously studied. We therefore examined early and late-
188 generation *prg-1* mutants grown at 20°C across several generations for activation of the
189 DNA damage response, as detected by an antibody to phosphorylated S/TQ, a protein
190 modification that is created by two sensors of DNA damage, ATM and ATR, which are
191 phosphatadylisonisol-3-kinase like protein kinases (Kim et al., 1999; Vermezovic et al.,
192 2012). We observed a significant increase in the fraction of germ cells with upregulated
193 DNA damage response for late-generation fertile and sterile *prg-1* mutants (~3- to 6-
194 fold) when compared to either wild type controls or to early-generation *prg-1* mutants
195 (Fig. 1A,B). However, the fraction of germ cells with an activated DNA damage
196 response was not consistently elevated in sterile *prg-1*/Piwi mutants in comparison to
197 fertile late-generation siblings (Fig. 1B). We also tested temperature-sensitive Piwi
198 pathway mutants and found that the wild-type DNA damage response was upregulated
199 by growth at 25°C but that this level was not further elevated in germlines of sterile late-
200 generation *rsd-6, nrde-2* or *hrde-1* mutant adults (Fig. 1B,C).

201

202 **Piwi pathway genome silencing mutants exhibit germ granule defects at sterility**

203 If secondary siRNAs are depleted from *prg-1* mutants and then restored by
204 crossing distinct *prg-1; mutator* double mutants together, this causes immediate sterility
205 for *prg-1* mutant F1 cross progeny that possess germ cells with germ granule defects

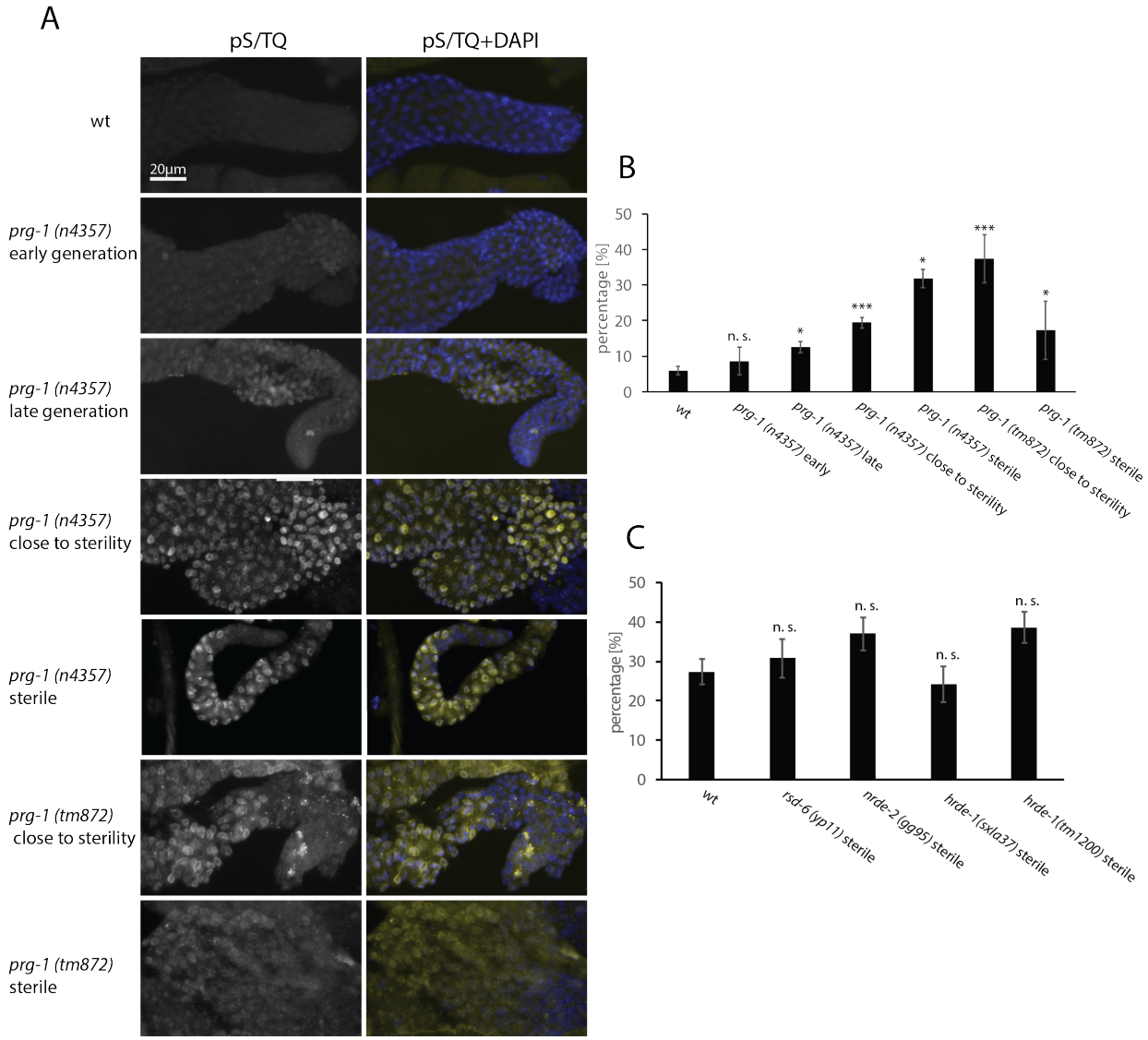

Figure 1: DNA Damage Response is variable in Piwi pathway genome silencing mutants prior to and at sterility. (A) Staining of pS/TQ in wild type, *prg-1(n4357) and prg-1(tm876)* mutants. pS/TQ(grey and yellow) and DAPI(blue) **(B)** Quantification of pS/TQ staining in 20°C wild type and *prg-1* mutants at different levels of fertility. **(C)** Quantification of pS/TQ staining in 25°C wild type and small RNA genomic silencing mutants at sterility. P-values were obtained by comparing sample groups in a Mann-

213 Whitney U test (p-value: P > 0.05 = n. s., P < 0.05 = *, P = <0.01 = **, P =< 0.001 = ***
214 compared to wild type).
215
216 and a range of adult germline sizes that are similar to those of sterile late-generation
217 Piwi pathway mutants (de Albuquerque et al., 2015; Phillips et al., 2015). Furthermore,
218 combined loss of the epigenomic regulators SPR-5 and LET-418, or loss of H3K9
219 methylation modifier SET-2 and the nuclear RNAi pathway, results in immediate sterility
220 that is associated with disruption of germ granules (P granules in *C. elegans*) (Käser-
221 Pébernard et al., 2014; Robert et al., 2014). Although most Piwi pathway mutants do not
222 display severe fertility defects until the generation of sterility, late-generation *prg-1*/Piwi
223 mutants display very small brood sizes for many generations prior to sterility (Heestand
224 et al., 2018). By immunofluorescence with a P granule antibody, we observed that P
225 granules were frequently strongly reduced or absent in nuclei of sterile late-generation
226 *prg-1* mutant germ cells (hereafter referred to as marked P granule dysfunction) (Fig.
227 2B, S1, Table 1), which was less common in fertile *prg-1(n4357)* mutant siblings while
228 *prg-1(tm872)* mutants showed more consistent P granule defects right before and at
229 sterility (Fig. 2B-B', Table 1). Consistently, growth of the temperature-sensitive Mrt
230 mutants *rsd-6*, *nrde-2*, *hrde-1* and *rbr-2* at the restrictive temperature of 25°C resulted in
231 sterile late-generation animals with marked P granule dysfunction, whereas their fertile
232 late-generation siblings did not exhibit pronounced P granule defects (Fig. 2C, D, E, C',
233 D', E', S1, Table 1).
234 Germ line atrophy occurs for many but not all sterile Piwi pathway mutants as L4
235 larvae develop into adults (Billmyre et al., 2019; Heestand et al., 2018). Large-scale

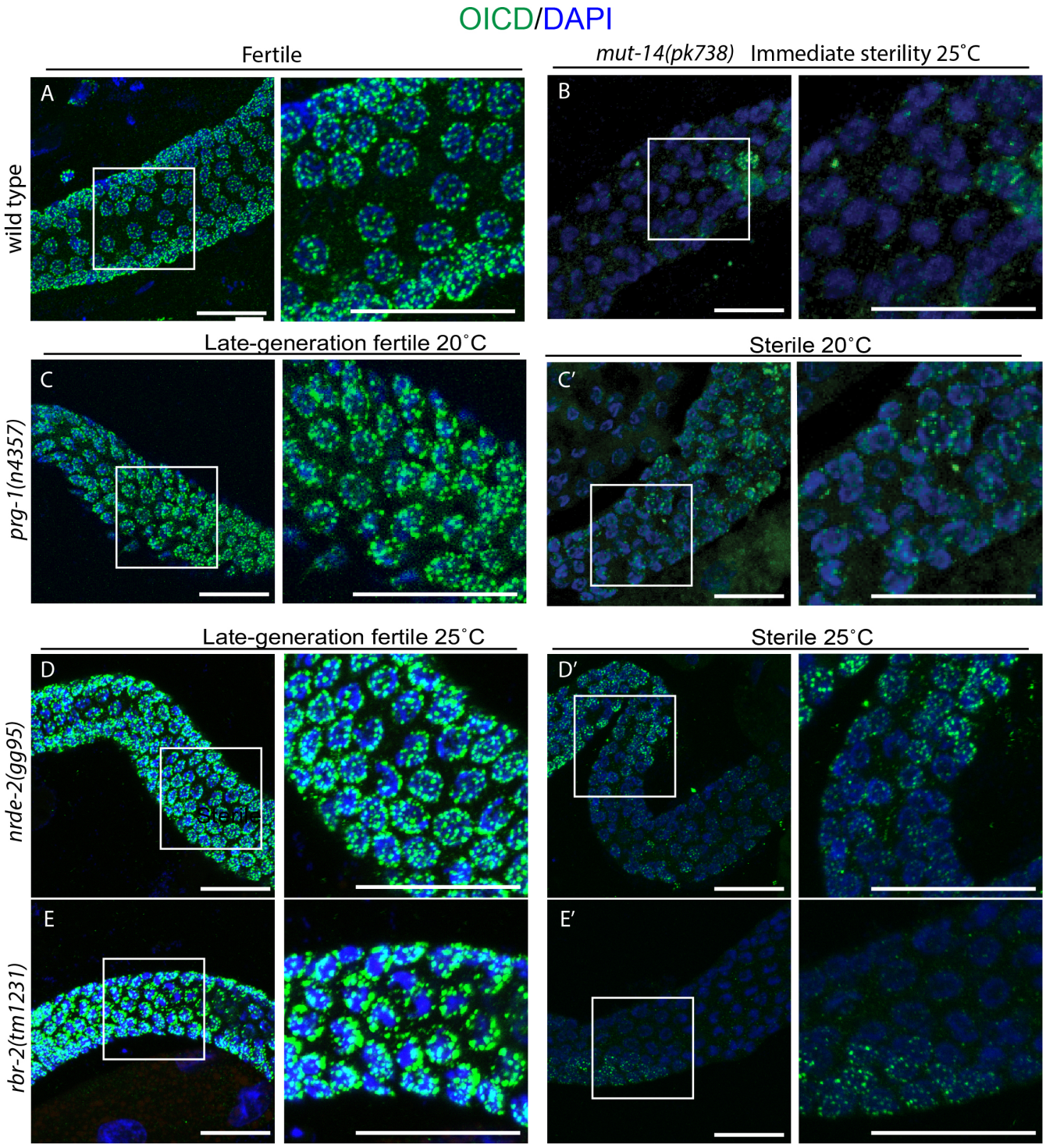
OICD/DAPI
Fertile
mut-14(pk738) Immediate sterility 25˚C
wild type
A
B
Late-generation fertile 20˚C
Sterile 20˚C
prg-1(n4357)
C
C′
Late-generation fertile 25˚C
Sterile 25˚C
nrde-2(gg95)
D
D′
Stem
rbr-2(tm1231)
E
E′

236

237

238 **Figure 2: At sterility, partial loss of P granule staining occurred in *prg-1* and**
239 **temperature-sensitive mutants.** Germlines of sterile Day 2-3 adult animals were
240 stained using the OIC1D4 antibody against P granules (green) and DAPI (blue). **(A)**
241 Control animals contain uniform puncta of P granule staining surrounding each
242 nuclei.(B) *mut-14* mutants display an immediate sterility when shifted to 25˚C for one
243 generation and display P granule abnormalities **(C-E)** Late generation fertile *prg-1,nrde-*
244 *2* and *rbr-2* animals displayed relatively normal P granule staining in the germlines. **(C'-**
245 **E')** *prg-1*, *nrde-2 and rbr-2* sterile animals all exhibited some degree of germ cell P
246 granule loss.
247
248 apoptosis contributes to but is not essential for this germ cell degeneration phenotype
249 (Heestand et al., 2018), and P granules have been shown to vanish in cells that
250 undergo apoptosis (Min et al., 2016; Sung et al., 2017). However, we observed marked
251 P granule dysfunction in germlines of sterile late-generation *nrde-2* and some *rsd-6*
252 mutant adults that were wild type in size and had not undergone significant amounts of
253 apoptosis (Fig. 2D, D'; Fig. S1F, F'). *nrde-1* and *nrde-4* mutant animals displayed a
254 sterility phenotype where many sterile germline arms displayed P granule defects (90%
255 and 87% respectively) (Fig. S1, Table 1). P granule defects in *nrde* mutants included P
256 granule dissociation from the nuclear envelope into the cytoplasm and P granule
257 aggregations as well as P granule loss. Therefore, dysfunction of *nrde-1* and *nrde-4*,
258 which act downstream of multiple small RNA genome silencing pathways (Fig. 6A),
259 might influence P granules differently than we observed in the germline arms of most
260 sterile Piwi pathway mutants.

261 *C. elegans* P granules are adjacent to Mutator bodies, which house Mutator
262 proteins that recruit RNA-dependent RNA polymerase to create secondary effector
263 siRNA populations in response to primary siRNAs (Phillips et al., 2012). *mutator*
264 mutants are dysfunctional for secondary siRNA biogenesis and remain fertile indefinitely
265 at low temperatures (Simon et al., 2014b), but display an immediate highly penetrant
266 fertility defect at 25°C that could be caused by dysfunction of Piwi pathway-mediated
267 heterochromatin (Ketting et al., 1999). We examined germlines of sterile *mut-14(pk738)*
268 mutant adults at the restrictive temperature of 25°C and observed pronounced P
269 granule defects in 66.67% of animals with no offspring and 100% P granule defects in
270 animals that laid eggs that could not develop into adults, here referred to as 'fertile'(Fig.
271 2B', Table 1).
272

273 **Germ granule dysfunction phenocopies sterile Piwi pathway genome silencing**
274 **mutants**

275 We addressed the significance of P granule dysfunction in sterile late-generation small
276 RNA genome silencing mutants using an RNA interference clone that simultaneously
277 targets four P granule subunits *pgl-1*, *pgl-3*, *glh-1*, *glh-4* (Fig. 6A) (Knutson et al., 2017;
278 Updike et al., 2014). This resulted in many second generation (G2) sterile adults at
279 25°C (80%) (Fig. 3A). The germlines of G2 P granule RNAi L4 larvae were normal in
280 size in comparison to control worms. However, a pronounced germ cell atrophy
281 phenotype occurred as many P granule-depleted animals matured into sterile adults,
282 resulting in a significant change in their germline profile (Fig. 3B, p=3.93E-24).

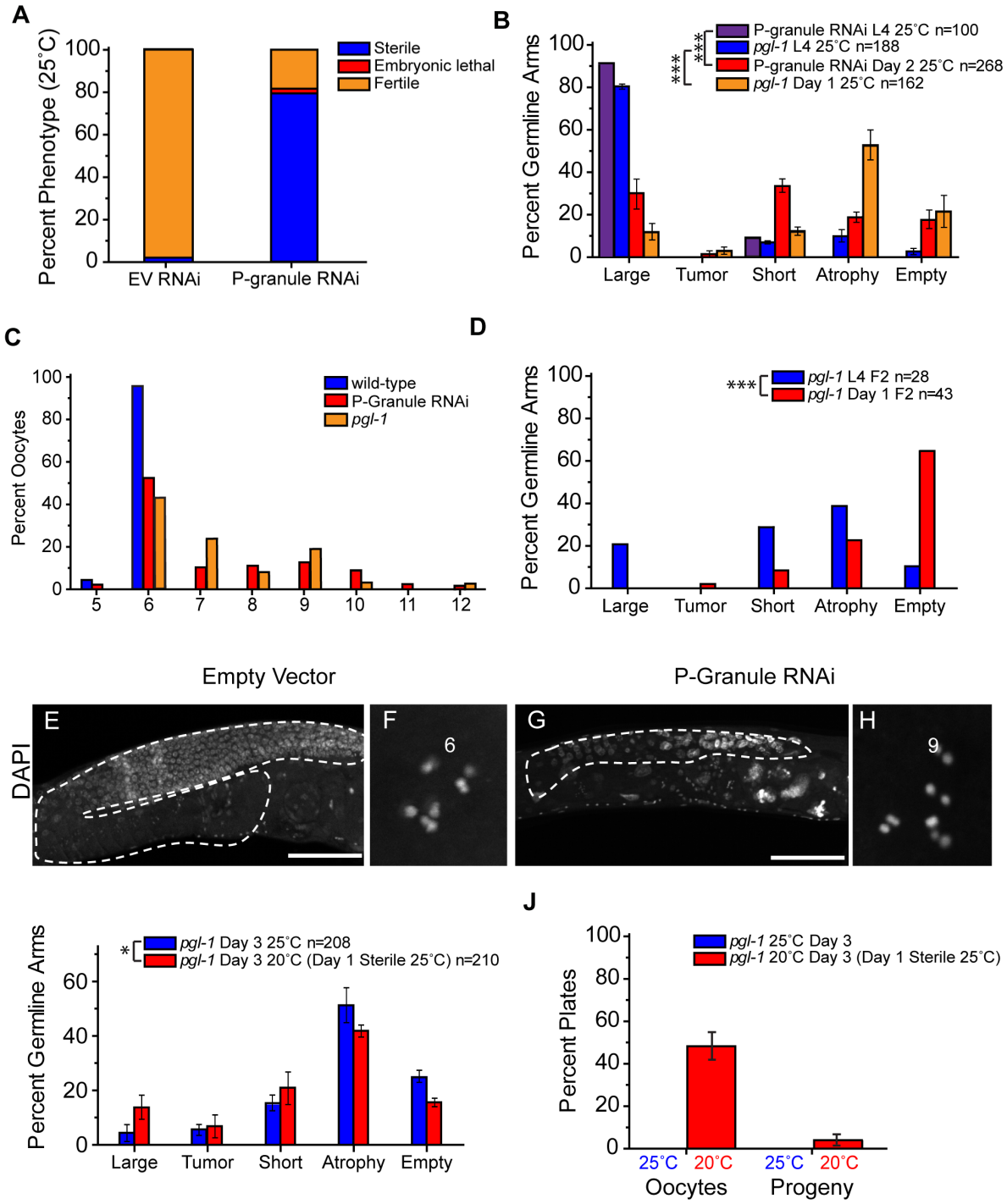

283

284 **Figure 3: Disruption of P granules by RNAi or by deficiency for *pgl-1* results in**

285 **similar phenotypes. (A)** G2 wildtype (N2) worms on Empty Vector (EV) or P granule

286 RNAi at 25°C were scored for sterility, embryonic lethality, or fertility. n=16-30 worms

287 per condition, 2 independent experiments. **(B)** Germline phenotypes of G1 L4 *pgl-1*
288 mutants and G2 L4 P granule RNAi treated animals stained by DAPI. **(C)** G1 *pgl-1*
289 mutants and G2 P granule RNAi treated animals contained oocytes with increased
290 numbers of univalents at sterility as measured by DAPI bodies n=151 wild type, 81 P
291 granule RNAi, 37 *pgl-1*. **(D)** Stained DAPI germlines of sterile G2 L4 and Day 1 *pgl-1*
292 mutants. **(E-H)** Representative DAPI images of germline and oocyte defects in empty
293 vector treated animals **(E,F)** and P granule RNAi treated animals **(G,H)** scale
294 bar=10µm. **(I)** *pgl-1* G1 worms at 25°C were either DAPI stained as Day 3 adults (blue)
295 or shifted to 20°C at Day 1 and DAPI stained at Day 3 (red). **(I)** No sterile day 1 *pgl-1*
296 G1 at 25°C laid oocytes or progeny (n=35 plates, 350 worms). Sterile day 1 *pgl-1*
297 shifted to 20°C (n=50 plates, 500 worms) gave rise to plates with oocytes and rarely
298 progeny. Plates with oocytes contained both oocytes and dead embryos. Plates with
299 progeny contained embryos that hatched to L1. For B,D,I *** $p<0.0001$, * $p=0.007$
300 Fisher's Chi Square test with Bonferroni correction, n=total germline arms scored, error
301 bars are S.E.M.
302
303 Furthermore, oocyte univalents were previously observed in sterile but not fertile late-
304 generation *rsd-6* mutants (Sakaguchi et al., 2014), and 45.5% of oocytes of sterile P
305 granule depleted adults contained 7-12 univalents (Fig. 3C, E-H), consistent with a
306 previous report (Billmyre et al., 2019).
307 The germline phenotypes observed in P granule-depleted worms mimicked those
308 of sterile *prg-1*/Piwi mutant adults (Fig. 3A-C), which can regrow their atrophied
309 germlines and become fertile (Heestand et al., 2018). We tested the hypothesis that

310 germ granule dysfunction might be sufficient to cause reproductive arrest using a
311 mutant deficient for the P granule component *pgl-1*, which remains fertile at low
312 temperatures but displays a pronounced sterility phenotype if shifted to the restrictive
313 temperature of 25°C (Kawasaki et al., 1998). Most first generation (G1) *pgl-1* animals at
314 25°C displayed normal germlines at the L4 larval stage, but there was a significant shift
315 in the germline profiles with 52% of day 1 adults showing germline atrophy (Fig. 3B,
316 p=1.04E-35), similar to P granule RNAi knockdown and sterile *prg-1* mutants (Heestand
317 et al., 2018). Furthermore, when oocytes of sterile *pgl-1* mutant adults were scored, we
318 found that 56.7% of oocytes had univalents, in agreement with the oocyte univalents
319 observed in response to P granule depletion by RNAi (Fig. 3C).

320 Some G1 progeny of *pgl-1* mutants whose parents were shifted from 20°C to
321 25°C were fertile and gave rise to G2 25°C animals that were uniformly sterile. 25°C G2
322 *pgl-1* mutant L4 larvae had germline profiles that displayed more severe germ cell
323 proliferation defects than those of G1 L4 larvae, and day 1 adults showed a striking 54%
324 increase in empty germlines (Fig. 3D, p=2.44E-05). Therefore, germlines of G1 progeny
325 of *pgl-1* mutant mothers that were shifted to the restrictive temperature of 25°C for a
326 single generation mimicked the germ cell degeneration phenotypes of sterile Piwi
327 pathway mutants as L4 larvae matured into adults, whereas 25°C G2 generation *pgl-1*
328 mutant larvae displayed more pronounced germ cell proliferation defects.

329 We asked if the fertility of sterile 25°C G1 *pgl-1* mutants could be restored by
330 shifting them to the permissive temperature of 20°C. Sterile G1 *pgl-1* mutants that
331 lacked embryos were shifted to 20°C on day 1 of adulthood and their germlines were
332 scored after 48 hours, which revealed a significant change in their germline profiles

333 (p=0.007), with a shift from atrophied germlines towards large germlines when
334 compared to sterile G1 *pgl-1* sibling controls that remained sterile at 25°C (Fig. 3I). In
335 agreement with the regrowth of some germline arms, we observed that some sterile G1
336 *pgl-1* mutant adults that were shifted to 20°C for several days had laid oocytes and
337 dead embryos, and that a few even gave rise to progeny (Fig. 3J). In contrast, sterile
338 *pgl-1* mutant control adults that were kept at 25°C never gave rise to oocytes, dead
339 embryos or living progeny (Fig. 3J).
340

341 **Transcriptional consequences of germ granule dysfunction and small RNA**
342 **genome silencing mutant sterility**

343 The sterility of Piwi/piRNA mutants correlates with expression of transposons and
344 associated genome instability (Brennecke et al., 2008b; Juliano et al., 2011; Kelleher,
345 2016; Siomi et al., 2011). We therefore studied RNA from the nuclear RNAi defective
346 mutants *nrde-1*, *nrde-2* and *nrde-4* (Buckley et al., 2012; Guang et al., 2008, 2010) that
347 have Mortal Germlines at 25°C (Burkhart et al., 2011). However, at 20°C *nrde-1* and
348 *nrde-4* mutants become progressively sterile but *nrde-2* mutants remain fully fertile
349 indefinitely (Burkhart et al., 2011). *nrde-1* and *nrde-4* mutants have relatively large
350 brood sizes at sterility at 20°C, such that large cohorts of L4 larvae that are poised to
351 become sterile can be collected. In contrast, *prg-1* mutants develop very low brood
352 sizes in late generations (Heestand et al., 2018), which makes it difficult to obtain many
353 synchronous animals that are poised to become sterile. We therefore prepared RNA
354 from early-generation and sterile-generation *nrde-1* and *nrde-4* mutants at 20°C and
355 compared this with RNA from wild type and *nrde-2* mutant controls.

356 We found that sterile generation *nrde-1* and *nrde-4* mutant L4 larvae showed
357 strong upregulation of similar transposon classes in comparison to early generation
358 *nrde-1* or *nrde-4* mutant L4 larvae or to wild type controls (Fig. 5A). We identified 18
359 transposon classes that were upregulated at least two-fold in both *nrde-1* and *nrde-4*,
360 13 of which were CER retrotransposons, which is consistent with previous
361 transgenerational analysis of *hrde-1* mutants (Ni et al., 2016). However, we also found
362 that *nrde-2* mutant controls that do not become sterile at 20°C displayed strong
363 upregulation of similar transposon loci, even in early generations. Of the 18 transposons
364 upregulated in both *nrde-1* and *nrde-4*, 17 were also upregulated in *nrde-2* compared
365 with wild type. Previous work reported that distinct classes of transposons are
366 upregulated in *prg-1* and *nrde-2* mutants (Das et al., 2008; McMurchy et al., 2017; Ni et
367 al., 2016; Simon et al., 2014b). Consistently, we analyzed published RNA-seq data from
368 *prg-1(n4357)* mutant animals (McMurchy et al., 2017) found that MIRAGE1 was the only
369 transposon upregulated in both *nrde-1*, *nrde-4* and *prg-1* mutants (McMurchy et al.,
370 2017) (Fig. 4A). Therefore, although deficiency for *prg-1* and *nrde-1/nrde-4* disrupts
371 small RNA-mediated genome silencing and compromises germ cell immortality, these
372 genes have distinct functions with regards to small RNA-mediated regulation of the
373 genome.

374 We compared gene expression data from sterile generation *nrde-1* or *nrde-4*
375 mutant L4 larvae with late-generation *prg-1* mutants (McMurchy et al., 2017) and with
376 wild type or *nrde-2* mutant control L4 larvae in order to identify common genes whose
377 expression is specifically induced in *nrde* mutant L4 larvae that are poised to become
378 sterile and that might explain the P granule abnormalities at sterility. Late-generation

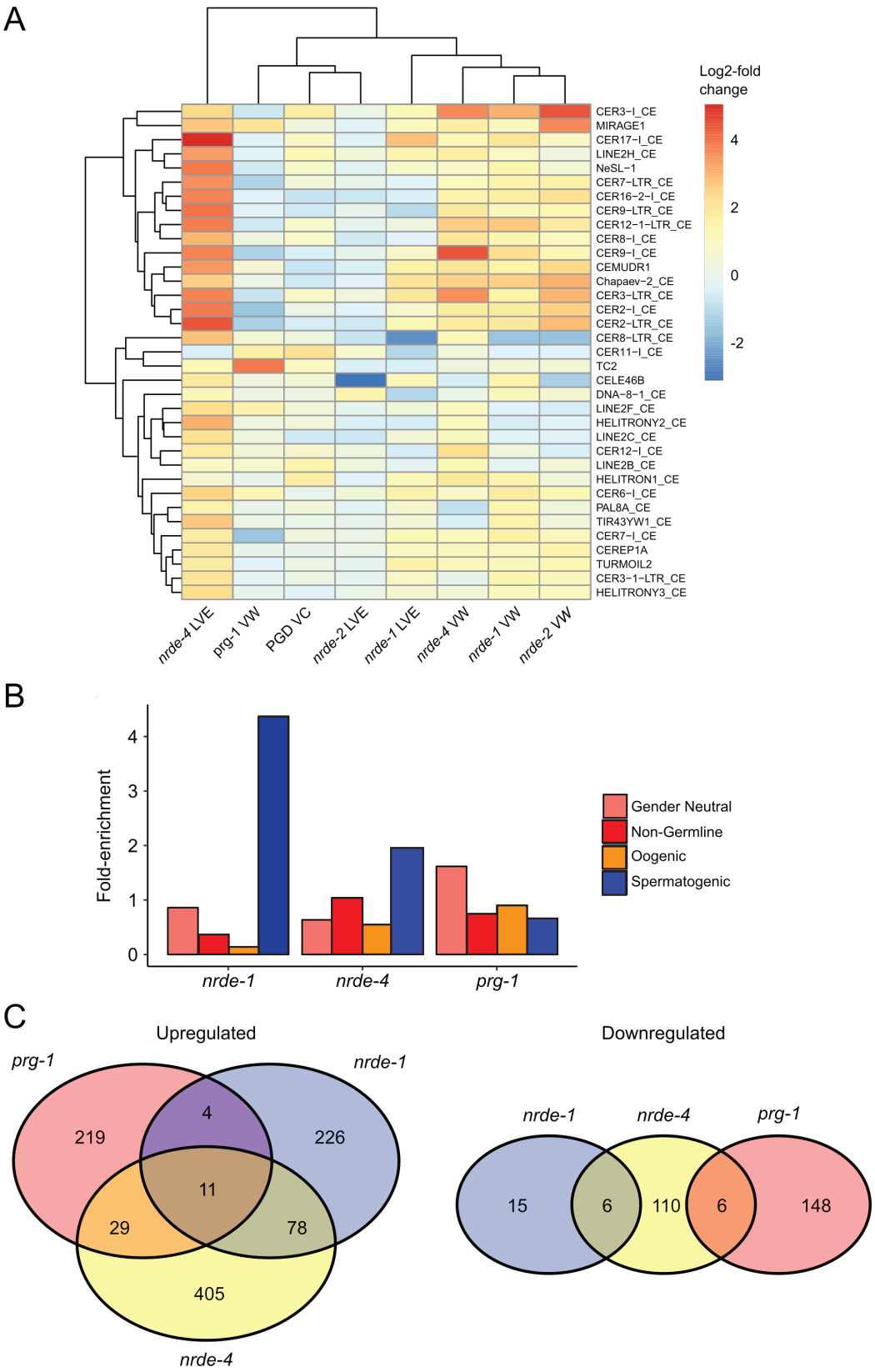
A
Log2-fold change
4
2
0
-2
CER3−I_CE
MIRAGE1
CER17−I_CE
LINE2H_CE
NeSL−1
CER7−LTR_CE
CER16−2−I_CE
CER9−LTR_CE
CER12−1−LTR_CE
CER8−I_CE
CER9−I_CE
CEMUDR1
Chapaev−2_CE
CER3−LTR_CE
CER2−I_CE
CER2−LTR_CE
CER8−LTR_CE
CER11−I_CE
TC2
CELE46B
DNA−8−1_CE
LINE2F_CE
HELITRONY2_CE
LINE2C_CE
CER12−I_CE
LINE2B_CE
HELITRON1_CE
CER6−I_CE
PAL8A_CE
TIR43YW1_CE
CER7−I_CE
CEREP1A
TURMOIL2
CER3−1−LTR_CE
HELITRONY3_CE
nrde-4 LVE
prg-1 VW
PGD VC
nrde-2 LVE
nrde-1 LVE
nrde-4 VW
nrde-1 VW
nrde-2 VW
B
Fold-enrichment
0
1
2
3
4
nrde-1
nrde-4
prg-1
Gender Neutral
Non-Germline
Oogenic
Spermatogenic
C
Upregulated
prg-1
nrde-1
nrde-4
219
4
226
11
29
78
405
Downregulated
nrde-1
nrde-4
prg-1
15
6
110
6
148

379

380 **Figure 4: Transcriptome profiling of germ granule deficient larvae of Piwi pathway**
381 **genome silencing mutants *nrde-1* and *nrde-4*. (A)** Log2-fold changes in transposon
382 transcript abundance in mutant vs wild type (VW), late vs early generation (LVE) or P
383 granule RNAi-treated vs control (PGD VC). Transposons upregulated at least two-fold in
384 *nrde-1*, *nrde-4* or *prg-1(n4357)* are shown. **(B)** Enrichment of germline-expressed genes
385 in genes upregulated in *nrde-1* and *nrde-4* mutants. **(C)** Number of genes up and
386 downregulated in *nrde-1* and *nrde-4* mutants.
387
388 *prg-1* mutant and sterile generation *nrde-1* and *nrde-4* mutant gene expression was
389 very different from wild type or *nrde-2* mutant controls RNA. Spermatogenic genes were
390 over-represented among genes significantly upregulated in sterile generation *nrde-1*
391 and *nrde-4* mutant larvae (p = 1e-15, Chi Square test for both mutants), which is
392 consistent with what has been previously reported for *spr-5* mutants that become
393 progressively sterile (Katz et al., 2009). However, there was no general tendency of an
394 up- or down-regulation of any gene category for *prg-1*, *nrde-1* and *nrde-4* mutants. Only
395 11 genes were significantly upregulated in all three mutants, and there were no
396 commonly downregulated genes, which suggests that *prg-1* and *nrde-1/nrde-4* mutants
397 have fundamentally different gene expression profiles at or near sterility (Fig. 4C). We
398 identified a set of 20 genes that were significantly upregulated at least fourfold in *prg-1*
399 and either *nrde-1* or *nrde-4*, which included *pud* (protein upregulated in dauer) genes
400 that might be consistent with a role for DAF-16/Foxo in *prg-1* mutant sterility (Table S2)
401 (Buckley et al., 2012; Simon et al., 2014a). However, we could not find consistent
402 changes in any gene whose knockdown perturbs P granule structure (Updike and

403 Strome, 2010), which suggests that altered germ granule structure of sterile Piwi
404 pathway mutants is a post-transcriptional response.
405 RNA-seq data sets were previously obtained for germlines of P granule defective
406 L4 larvae that were poised to become sterile, but gene expression was not significantly
407 different from wild type (Knutson et al., 2017). We compared RNA from germlines of P
408 granule defective L4 larvae (Knutson et al., 2017) with RNA from sterile generation
409 *nrde-1* and *nrde-4* L4 larvae and found no genes that were up or downregulated in both
410 *nrde-1/nrde-4* and P granule defective larvae. Moreover, only two of 18 transposons
411 upregulated in *nrde-1/nrde-4* were also upregulated in P granule defective L4 larvae
412 (Fig. 4A). We conclude although acute dysfunction of P granules based on
413 simultaneous knockdown of four P granule components leads to germ line degeneration
414 phenotypes that mimic those of sterile generation Piwi pathway mutants, it does not
415 cause immediate overt effects on expression of heterochromatic segments of the
416 genome or on genes in a manner that mimics the transcriptomes of Piwi pathway
417 mutants that are poised to become sterile. Interestingly, the differences between *nrde-*
418 *1/nrde-4* RNA data and *prg-1* also correlate with differences that we observed in P
419 granule abnormalities between these mutants (Figure 2, S1). This indicates that the
420 sterility observed in nrde and PIWI mutants causes P granule defects resulting from
421 different molecular pathways.
422
423 **Deficiency for *pgl-1* enhances *prg-1*/Piwi mutant sterility**
424 Given that deficiency for *pgl-1* or RNAi knockdown of P granule components at 25°C
425 mimics Piwi mutant sterility, we performed an RNAi screen for P granule components

426 whose knockdown induces sterility in early-generation *prg-1* mutants or in *pgl-1* mutants
427 grown at the permissive temperature of 20°C. We knocked down several P-granule
428 components for 10 generations in wild type control animals and in strains deficient for
429 either *prg-1* or the P-granule component *pgl-1* (Fig 5A). Several RNAi clones led to
430 immediate sterility for all genotypes tested, and we also identified P granule
431 components whose knockdown induced sterility the *pgl-1* mutant. Specifically, we found
432 that RNAi of *prg-1*/Piwi induced sterility in *pgl-1* mutants in generation F4 (Fig 5B). We
433 studied the germline phenotypes of sterile *pgl-1* mutants treated with *prg-1* RNAi and
434 observed that they had a mixture of empty, atrophied and short germlines (Fig. 5B, D).
435 To confirm the interaction of *pgl-1* mutation with RNAi knockdown of *prg-1*, we
436 used outcrossed mutations in *prg-1* and *pgl-1* to create *prg-1; pgl-1* double mutants and
437 compared them to the single mutant outcrossed controls. We found that *prg-1* (20/20)
438 and *pgl-1* (20/20) single mutant controls were fertile for 10 generations when grown at
439 20°C. In contrast, *prg-1; pgl-1* double mutant F2 adults were fertile but gave rise to F3
440 animals that were almost all sterile (41/45) (Fig 5C). We stained sterile *prg-1; pgl-1*
441 double mutant F3 with DAPI and found that on Day 1 62.9% of germlines were either
442 atrophied or empty (Fig 5B).
443
444 **Discussion:**
445 Previous work has demonstrated that Piwi mutant sterility correlates with transposon
446 expression, transposition and genomic instability in several species (Juliano et al., 2011;
447 Kelleher, 2016; Siomi et al., 2011). We studied DNA damage signaling in *C. elegans*
448 Piwi pathway mutants and found that this was not consistently increased in sterile

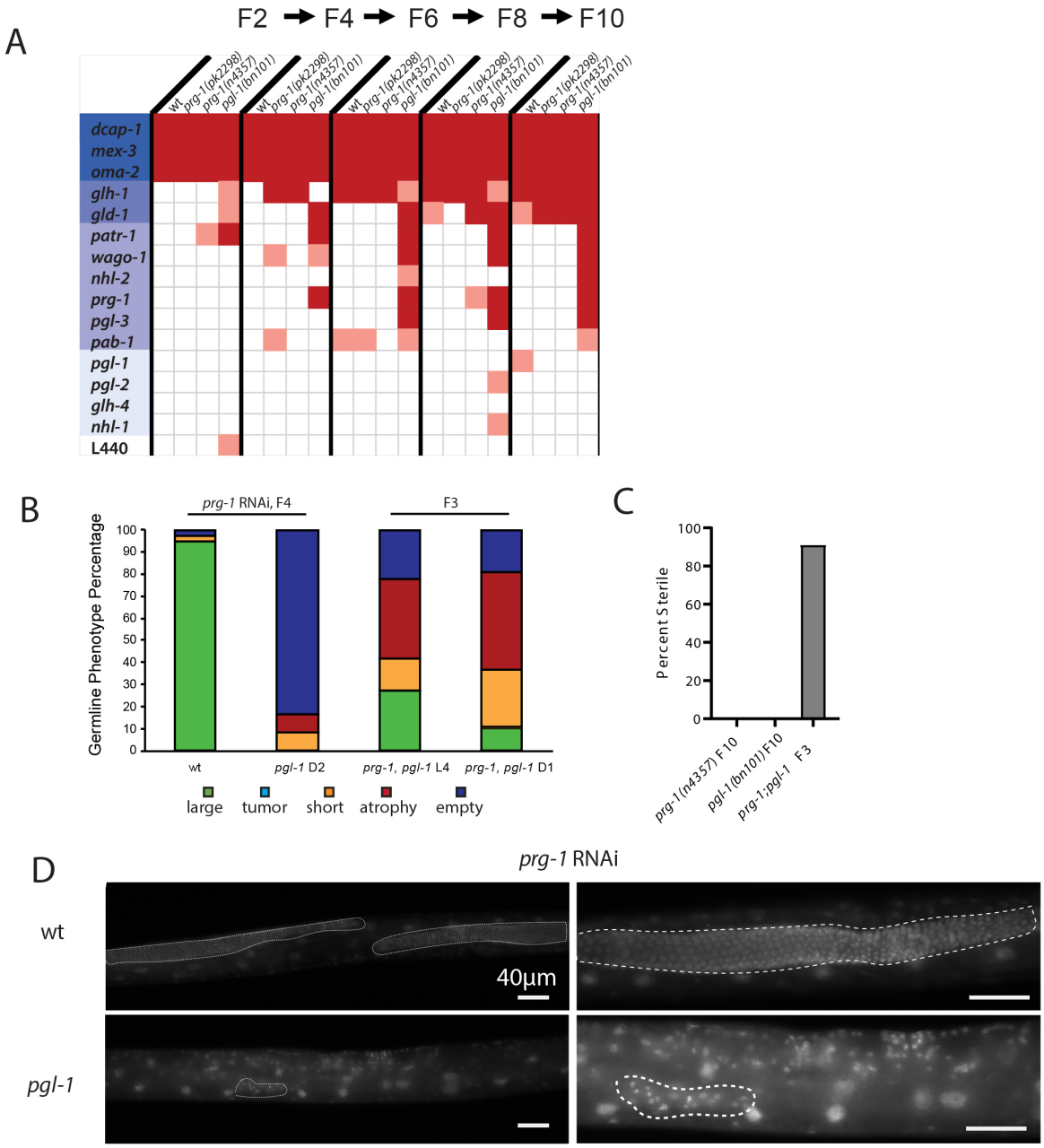

449

450 **Figure 5: Deficiency for *pgl-1* results in rapid sterility of *prg-1* mutants.** (A)

451 Germline immortality assay with wild type, *prg-1(pk2298), prg-1(n4357)* and *pgl-*

452 *1(bn101)* on different P-granule RNAi clones. 2 replicates of 3 L1 larvae were

453 transferred every week or after 2 generations and plates were scored as sterile when no

454 more than 3 worms were present after 1 week. Light red indicates sterility for 1 of 2
455 replicate plates while dark red indicates sterility for both replicates. When one plate
456 became sterile worms from the second plate were used for 2 replicates. (B) Germline
457 sizes of wild type and *pgl-1(bn101)* on *prg-1* RNAi after 4 generations and of *prg-1; pgl-*
458 *1* double mutant F3 animals. (C) *prg-1; pgl-1* double mutants display marked sterility in
459 the F3 generation.(D) Germline comparison of wild type and *pgl-1(bn101)* on *prg-1*
460 RNAi after 4 generations.
461
462 animals in comparison to fertile late-generation siblings. These data complement
463 previous observations that suggest that DNA damage induced by transposition is
464 unlikely to cause the transgenerational sterility of *prg-1*/Piwi mutants (Simon et al.,
465 2014b). A recent study revealed that defects in H3K9 methylation caused by *met-2* and
466 *set-25* histone methyltransferases cause R-loops and mutations at tandem repeats in
467 the *C. elegans* genome, reduced fertility, and synthetic sterility with the ATR homolog
468 *atl-1* (Padeken et al., 2019) However, the sterility of the Piwi mutants we studied was
469 not associated with high levels of ATR signaling, suggesting that Piwi sterility may be
470 distinct from the reduced fertility caused by loss of H3K9me2 and me3 (Padeken et al.,
471 2019).
472 We discovered pronounced germ granule defects in sterile but to a lesser extent
473 in fertile late-generation Piwi pathway mutants and tested their significance by
474 disrupting germ granule proteins (Fig. 3). We found that shifting a *pgl-1* germ granule
475 mutant to restrictive temperature, led to germline degeneration phenotypes that
476 phenocopied those of sterile generation Piwi pathway mutants (Heestand et al., 2018).

477 We also found that restoring germ granule function sterile *pgl-1* mutant adults, by
478 shifting them to the permissive temperature of 20°C, resulted in growth of the germline
479 and fertility (Fig. 3I-J).

480 Although sterility in response to germ granule dysfunction has previously been
481 considered to be a pathological condition that results in a germline-to-soma
482 transformation (Knutson et al., 2017), our results indicate that germ granule dysfunction
483 can induce reproductive arrest in adults (Fig. 3, 6C). As environmental stresses such as
484 starvation can also evoke reproductive arrest (Angelo and Van Gilst, 2009; Padilla and
485 Ladage, 2012), we speculate that germ granule dysfunction might represent a general
486 mechanism for orchestrating stress-induced reproductive arrest.

487 Sterile late-generation *prg-1*/Piwi pathway mutants display a broad range of
488 germline phenotypes that are observed in response to germ granule dysfunction,
489 including germ cell atrophy, empty germlines, univalent chromosomes in oocytes,
490 germline regrowth and reproductive arrest (Heestand et al., 2018). Together with the
491 germ granule defects observed in sterile Piwi pathway mutants, our results suggest that
492 Piwi mutant sterility is a form of reproductive arrest that may be caused by germ granule
493 dysfunction (Fig. 6B). If the germ granule defects in sterile Piwi pathway mutants were a
494 consequence rather than a cause of Piwi mutant sterility, then we would have expected
495 that disrupting germ granule function would lead to a distinct form of sterility that did not
496 bear hallmarks of Piwi mutant sterility like germ cell atrophy and reproductive arrest
497 (Fig. 6C). Another reason that germ granule defects of sterile Piwi pathway mutants are
498 unlikely to be a consequence of Piwi mutant sterility is that we observed some sterile
499 Piwi pathway mutants with large germlines that did not display obvious P granule

500 defects (Fig. 2, S1). We also found that deficiency for the P granule component *pgl-1*
501 dramatically accelerated the sterility in response to deficiency for *prg-1*/Piwi, indicating
502 that these proteins function redundantly to promote germ cell immortality. Knockdown of
503 the germ granule components *gld-1* and *pgl-3* also induced F4 generation sterility for
504 *pgl-1* mutants, which suggests a common function PRG-1, GLD-1 and PGL-3 in
505 promoting transgenerational fertility in the context of germ granules that is consistent
506 with their known physical interactions (Akay et al., 2013; Chen et al., 2016)

507 Although P granules and associated Mutator bodies contain proteins like PRG-
508 1/Piwi and a host of other factors that promote small RNA biogenesis (Billi et al., 2012),
509 we did not observe strong expression of heterochromatic transposons that are normally
510 silenced by small RNAs in L4 larvae that are poised to become sterile because of germ
511 granule dysfunction. This observation is consistent with the premise that small RNA-
512 induced genomic silencing marks can be maintained in the absence of small RNA
513 biogenesis.

514 Previous analysis showed that crosses that restored secondary siRNAs to *prg-1*
515 mutants created sterile F1 *prg-1/*Piwi mutant progeny that possessed adult germlines
516 with sizes analogous to those of sterile late-generation *prg-1* mutants and in disruption
517 of P granules (de Albuquerque et al., 2015; Heestand et al., 2018). This led to the
518 hypothesis that misrouting of small RNAs associated with pro- and anti-silencing small
519 RNA pathways could be the cause of sterility in Piwi pathway genome silencing mutants
520 (de Albuquerque et al., 2015; Phillips et al., 2015), which agrees with our observations
521 of germ granule abnormalities in sterile but not fertile late-generation Piwi pathway
522 mutants. Consistently, sterile mouse mutants with defects in piRNA biogenesis have

523 been reported to display germ granule defects (Chuma et al., 2006; Zheng and Wang,
524 2012). We suggest that germ granule dysfunction could explain the sterility observed in
525 P-M hybrid dysgenesis and the immediate sterility phenotype of Piwi mutants in several
526 species (Juliano et al., 2011; Kelleher, 2016; Siomi et al., 2011).

527 When RNA from sterile generation *nrde-1* and *nrde-4* mutant L4 larvae and late-
528 generation *prg-1*/Piwi mutants was examined, we failed to observe consistent depletion
529 of any gene whose knockdown is known to disrupt P granule formation (Updike and
530 Strome, 2010), suggesting a post-transcriptional reproductive arrest mechanism (Fig.
531 4B). We propose that transgenerational dysfunction of the Piwi/piRNA pathway in *C.*
532 *elegans* results in heterochromatin defects and transcription of 'stressful RNA' from one
533 or more genomic loci in later generations, which triggers a reproductive arrest program
534 that perturbs germ granule structure (Fig. 6B). A role for defective heterochromatin as a
535 cause of Piwi mutant sterility is supported by the *C. elegans* mutants *spr-5* and *rbr-2*,
536 which encode H3K4 demethylases that function within nuclei downstream of small
537 RNAs to promote genomic silencing (Fig. 2). *spr-5* and *rbr-2* mutants display
538 transgenerational sterility phenotypes that mirror those of Piwi pathway silencing
539 mutants (Alvares et al., 2014; Billmyre et al., 2019).

540 With regards to the model of telomerase deficiency as a cause of replicative
541 aging in mammalian cells, we suggest that germ granule dysfunction in Piwi mutants
542 may be analogous to telomere uncapping in the context of senescence (Sharpless and
543 DePinho, 2007; Shay and Wright, 2000). Acute germ granule dysfunction is sufficient to
544 mimic Piwi mutant sterility (Fig. 3, 6C), similar to knockdown of the TRF2 telomere
545 capping protein being sufficient to induce acute telomere uncapping and senescence

546 (Karlseder et al., 1999). In the case of replicative aging of mammalian cells, progressive
547 telomere erosion is the source of damage that ultimately induces telomere uncapping.
548 In the case of transgenerational Piwi pathway mutant sterility, it remains unclear what is
549 the precise source of 'heritable stress' that accumulates over generations to induce
550 sterility, although this is likely to be related to transgenerational desilencing of
551 heterochromatin/transposons (Fig. 5A).

552 Our results establish a novel framework for considering inheritance in the context
553 of epigenetic stress and how this can evoke sterility. We suggest that Piwi mutant
554 sterility is a response to epigenome dysfunction that arrests germ cell development in
555 an effort to protect the genome or epigenome in times of stress. Transposons and
556 viruses are likely to be in a continuous arms race between parasite and host, where
557 components of germ granules that promote Piwi pathway genome silencing and protect
558 the host are likely to be targeted (Updike and Strome, 2010). It may therefore be
559 reasonable to hypothesize the evolution of a reproductive arrest mechanism in the
560 context of an attack on the Piwi silencing system that is predicated on disrupting the
561 integrity of germ granules themselves.

562

563 **Materials and Methods**

564

565 Strains

566 All strains were cultured at 20°C or 25°C on Nematode Growth Medium (NGM) plates
567 seeded with *E. coli* OP50. Strains used include Bristol N2 wild type, *hrde-1(tm1200) III,*
568 *nrde-1(yp4) III, nrde-2(gg95) II, nrde-4 (gg131) IV, prg-1 (n4357) I, prg-1 (tm872) I, prg-*

569

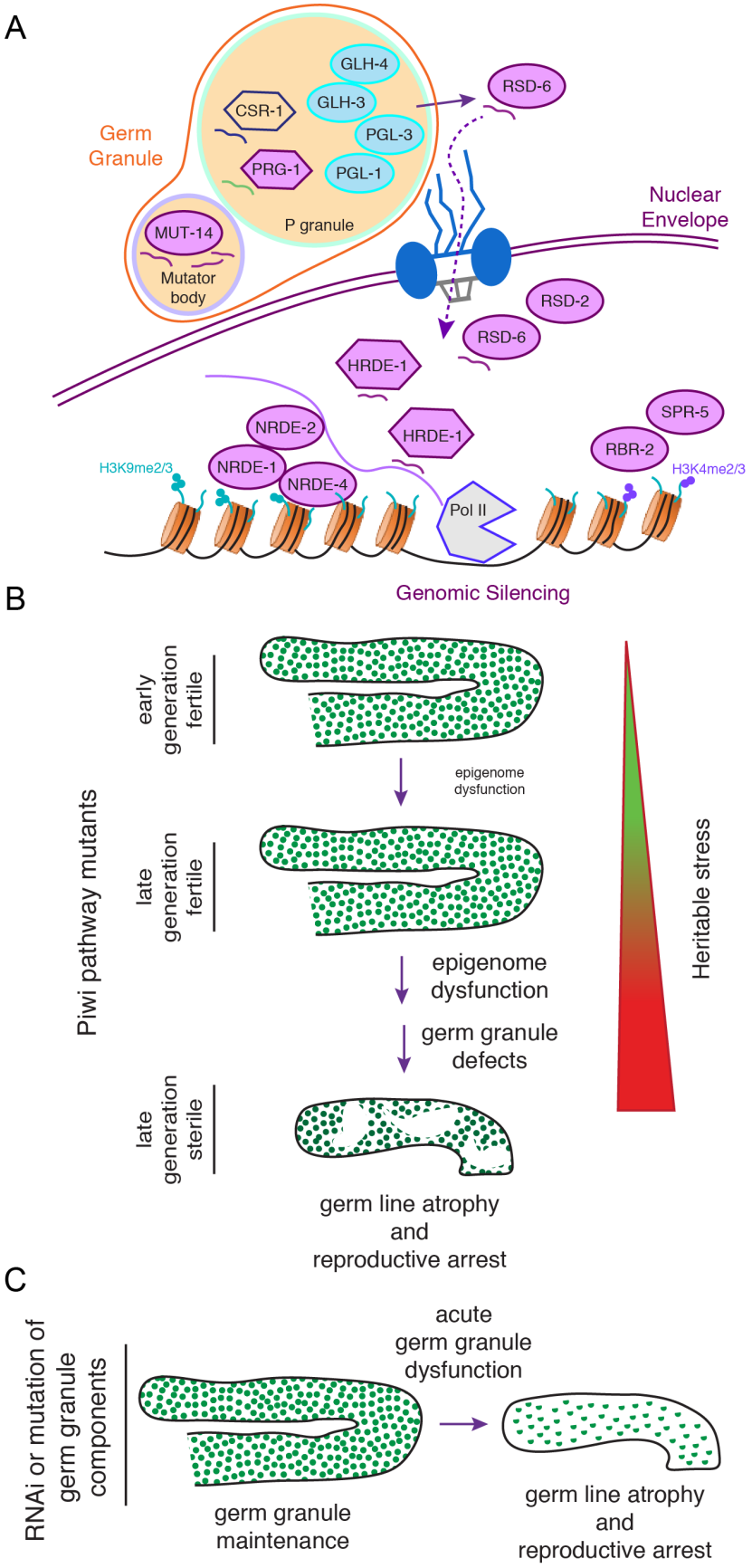
A
Germ Granule
GLH-4
GLH-3
CSR-1
PGL-3
PRG-1
PGL-1
P granule
MUT-14
Mutator body
RSD-6
Nuclear Envelope
RSD-2
RSD-6
HRDE-1
HRDE-1
NRDE-2
NRDE-1
NRDE-4
H3K9me2/3
SPR-5
RBR-2
H3K4me2/3
Pol II
Genomic Silencing
B
Piwi pathway mutants
early generation fertile
epigenome dysfunction
late generation fertile
epigenome dysfunction
germ granule defects
late generation sterile
germ line atrophy and reproductive arrest
Heritable stress
C
RNAi or mutation of germ granule components
acute germ granule dysfunction
germ granule maintenance
germ line atrophy and reproductive arrest

570

571 **Figure 6: Model for P granule dysfunction in Piwi pathway genome silencing**
572 **mutants.** (**A**) Model of P granules and associated small RNA-mediated genome
573 silencing proteins. Blue circles contain P granule components used in this paper.
574 Mutants used this paper are in lavender. Argonaute proteins are hexagons. Non-
575 conditional mutants have red outlines. **(B)** Model for transgenerational sterility in
576 response to accumulation of Heritable Stress in Piwi pathway genome silencing
577 mutants, which ultimately compromises P granule integrity. **(C)** Model for induction of
578 reproductive arrest by acute dysfunction of P granule components.
579
580 *1(pk2298) I, pgl-1(bn101) IV, mut-14 (pk738) V, rbr-2(tm1231) IV,* HIS-72::mNeonGreen
581 (LP230).
582
583 RNAi Assay
584 Feeding RNAi plates harboring host bacteria HT115(DE3) engineered to express *"*quad*"*
585 dsRNA (targeting *pgl-1*, *pgl-3*, *glh-1*, *glh-4*) were obtained from Susan Strome (Knutson
586 et al., 2017; Updike et al., 2014). L1 larvae were placed onto freshly prepared feeding
587 RNAi plates with dsRNA induced by 1 mM IPTG (isopropyl-β-D(-)-
588 thiogalactopyranoside) and were transferred after 1 generation at 25°C and collected at
589 G2 adults as described in Knutson et al 2017 (Knutson et al., 2017) for DAPI staining,
590 oocyte and germline analysis.
591 For RNAi screen, L1 worms containing the *his-72*:: *mNeonGreen* transgene were
592 arrested in M9 media and then pipetted at a density of 20 worms per plate and

593 maintained at 20°C. At the L4 stage and during adulthood worms were scored for
594 germline size using Leica M205 fluorescence microscope.
595 For the P-granule germline immortality assay 3 L1 worms were transferred every week
596 on two replicate plates per condition at 20˚C. Plates were counted as sterile when no
597 more than 3 worms were present after one week. Partial sterility was counted when one
598 out of two plates became sterile while both replicate plates were sterile for full sterility.
599

600 DAPI staining and Scoring

601 DAPI staining was performed as previously described (Ahmed and Hodgkin, 2000).
602 Briefly, L4 larvae were selected from sibling plates and sterile adults were singled as
603 late L4s, observed 24 hours later for confirmed sterility, and then stained 48 hours after
604 collection. Univalents were scored by counting DAPI bodies in the -1 to -4 oocytes.
605 Germline profiles were scored using the method outlined in Heestand et al 2018
606 (Heestand et al., 2018).
607

608 Statistical Analysis

609 Statistical analysis was performed as previously described (Heestand et al., 2018).
610 Briefly, statistical analysis was performed using the R statistical environment (R Core
611 Team, 2013). For germline phenotypes, contingency tables were constructed and
612 pairwise Chi Square tests with Bonferroni correction was used to determine significant
613 differences in in germline phenotype distributions. The significance of the DNA damage
614 response analysis was determined by a Kruskal-Wallis test, followed by a Mann-

615 Whitney test between individual samples. P-values were adjusted with Bonferroni
616 correction when multiple comparisons were performed.
617
618 RNA extraction and sequencing
619 Animals were grown at 20°C on 60 mm NGM plates seeded with OP50 bacteria. RNA
620 was extracted using Trizol (Ambion) followed by isopropanol precipitation. Library
621 preparation and sequencing was performed at the UNC School of Medicine High-
622 Throughput Sequencing Facility (HTSF). Libraries were prepared from ribosome-
623 depleted RNA and sequenced on an Illumina Hiseq 2500.
624
625 RNA-seq Analysis
626 The following publicly available RNA-seq datasets were download from the Gene
627 Expression Omnibus (https://www.ncbi.nlm.nih.gov/geo/): GSE92690 (P granule RNAi
628 experiment) and GSE87524 (*prg-1* experiment). Adapter trimming was performed as
629 required using the bbduk.sh script from the BBmap suite (Bushnell) and custom scripts.
630 Reads were then mapped to the *C. elegans* genome (WS251) using hisat2 (Kim et al.,
631 2013) with default settings and read counts were assigned to protein-coding genes
632 using the featureCounts utility from the Subread package (Liao et al., 2014) . For
633 multimapping reads, each mapping locus was assigned a count of 1/n where n=number
634 of hits. Differentially expressed genes were identified using DESeq2, and were defined
635 as changing at least 2-fold with FDR-corrected p-value < 0.01. For analysis of
636 transposon RNAs, reads were mapped to the *C. elegans* transposon consensus
637 sequences downloaded from Repbase (http://www.girinst.org/repbase/) with bowtie

638 (Langmead et al., 2009) using the options -M 1 -v 2. Transposons with fewer than 10
639 counts in each sample were excluded from further analysis. Counts were normalized to
640 the total number of mapped reads for each library for the prg-1 dataset, or to the total
641 number of non-ribosomal mapped reads for all other datasets. A pseudocount of 1 was
642 added to each value to avoid division by zero errors. Analysis of sequencing data and
643 plot creation was performed using the R statistical computing environment (R Core
644 Team, 2013).
645
646 Accession numbers: RNA-seq data reported in this study have been submitted to the
647 GEO database and will be available at the time of publication.
648
649 Immunofluorescence
650 Adult hermaphrodites raised at 20°C or 25°C were dissected in M9 buffer and flash
651 frozen on dry ice before fixation for 1 min in methanol at -20°C. After washing in PBS
652 supplemented with 0.1% Tween-20 (PBST), primary antibody diluted in in PBST was
653 used to immunostain overnight at 4 °C in a humid chamber. Primaries used were 1:50
654 OIC1D4 (Developmental Studies Hybridoma Bank). Secondary antibody staining was
655 performed by using a Cy3 donkey anti-mouse or Cy-5 donkey anti-rabbit overnight at
656 4°C. All images were obtained using a LSM 710 laser scanning confocal and were
657 taken using same settings as control samples. Images processed using ImageJ.
658 Marked P granule dysfunction was scored by eye as a loss of greater or less than 20%
659 loss of P granules.
660

661 DNA Damage Assay

662 Worms that were close to sterility were isolated and defined as sterile if they did not
663 have any offspring as day 3 adults at 20˚C or day 2 adults at 25˚C. Fertile siblings of
664 sterile worms were defined as 'close to sterility'. The presence of the DNA damage
665 response was determined by using a phospho-specific antibody targeting the
666 phosphorylated consensus target site of ATM and ATR kinases (pS/TQ) (Cell Signaling
667 Technology). This antibody has only been shown to stain a DNA damage response in
668 the germline and was used as previously described (Vermezovic et al., 2012).

669

670 **Acknowledgments:** We thank members of the Ahmed lab for critical reading of the
671 manuscript and Jacinth Mitchell for wild type control, *nrde-1* and *nrde-2* RNA-seq data.
672 Some strains were provided by the CGC, which is funded by NIH Office of Research
673 Infrastructure Programs (P40 OD010440). This study was supported by NIH grants F32
674 GM120809 (K.B) and RO1 GM083048 (S.A). M.S. was supported by a DFG postdoc
675 fellowship.

676

677 **Competing interests:** Authors declare no competing interests.

678

679 **Author contributions:** K.B., B.H., M.S. and S.F. performed experiments. S.F. analyzed
680 the data. K.B., B.H., M.S., S.F. and S.A. wrote manuscript.

681

682 **References:**

683 Ahmed, S., and Hodgkin, J. (2000). MRT-2 checkpoint protein is required for germline

684 immortality and telomere replication in C. elegans. Nature *403*, 159–164.

685 Akay, A., Craig, A., Lehrbach, N., Larance, M., Pourkarimi, E., Wright, J.E., Lamond, A.,
686 Miska, E., and Gartner, A. (2013). RNA-binding protein GLD-1/quaking genetically
687 interacts with the mir-35 and the let-7 miRNA pathways in Caenorhabditis elegans.
688 Open Biol. *3*, 130151–130151.

689 de Albuquerque, B.F.M., Placentino, M., and Ketting, R.F. (2015). Maternal piRNAs Are
690 Essential for Germline Development following De Novo Establishment of Endo-siRNAs
691 in Caenorhabditis elegans. Dev. Cell *34*, 448–456.

692 Alvares, S.M., Mayberry, G.A., Joyner, E.Y., Lakowski, B., and Ahmed, S. (2014). H3K4
693 demethylase activities repress proliferative and postmitotic aging. Aging Cell *13*, 245–
694 253.

695 Angelo, G., and Van Gilst, M.R. (2009). Starvation Protects Germline Stem Cells and
696 Extends Reproductive Longevity in C. elegans. Science (80-.). *326*, 954–958.

697 Aravin, A.A., Hannon, G.J., and Brennecke, J. (2007). The Piwi-piRNA pathway
698 provides an adaptive defense in the transposon arms race. Science *318*, 761–764.

699 Ashe, A., Sapetschnig, A., Weick, E.M., Mitchell, J., Bagijn, M.P., Cording, A.C.,
700 Doebley, A.L., Goldstein, L.D., Lehrbach, N.J., Le Pen, J., et al. (2012). PiRNAs can
701 trigger a multigenerational epigenetic memory in the germline of C. elegans. Cell *150*,
702 88–99.

703 Batista, P.J., Ruby, J.G., Claycomb, J.M., Chiang, R., Fahlgren, N., Kasschau, K.D.,
704 Chaves, D.A., Gu, W., Vasale, J.J., Duan, S., et al. (2008). PRG-1 and 21U-RNAs
705 Interact to Form the piRNA Complex Required for Fertility in C. elegans. Mol. Cell *31*,

706 67–78.

707 Billi, A.C., Freeberg, M.A., and Kim, J.K. (2012). piRNAs and siRNAs collaborate in
708 Caenorhabditis elegans genome defense. Genome Biol. *13*, 164.

709 Billmyre, K.K., Doebley, A.-L., Spichal, M., Heestand, B., Belicard, T., Sato-Carlton, A.,
710 Flibotte, S., Simon, M., Gnazzo, M., Skop, A., et al. (2019). The meiotic phosphatase
711 GSP-2/PP1 promotes germline immortality and small RNA-mediated genome silencing.
712 PLOS Genet. *15*, e1008004.

713 Bodnar, A.G., Ouellette, M., Frolkis, M., Holt, S.E., Chiu, C.P., Morin, G.B., Harley, C.B.,
714 Shay, J.W., Lichtsteiner, S., and Wright, W.E. (1998). Extension of life-span by
715 introduction of telomerase into normal human cells. Science *279*, 349–352.

716 Brennecke, J., Malone, C.D., Aravin, A.A., Sachidanandam, R., Stark, A., and Hannon,
717 G.J. (2008a). An epigenetic role for maternally inherited piRNAs in transposon silencing.
718 Science *322*, 1387–1392.

719 Brennecke, J., Malone, C.D., Aravin, A.A., Sachidanandam, R., Stark, A., and Hannon,
720 G.J. (2008b). An Epigenetic Role for Maternally Inherited piRNAs in Transposon
721 Silencing. Science (80-.). *322*, 1387–1392.

722 Buckley, B.A., Burkhart, K.B., Gu, S.G., Spracklin, G., Kershner, A., Fritz, H., Kimble, J.,
723 Fire, A., and Kennedy, S. (2012). A nuclear Argonaute promotes multigenerational
724 epigenetic inheritance and germline immortality. Nature *489*, 447–451.

725 Burkhart, K.B., Guang, S., Buckley, B.A., Wong, L., Bochner, A.F., and Kennedy, S.
726 (2011). A pre-mRNA-associating factor links endogenous siRNAs to chromatin
727 regulation. PLoS Genet. *7*, e1002249.

728 Bushnell, B. BBMap short-read aligner.

729 Chen, J.-X., Cipriani, P.G., Mecenas, D., Polanowska, J., Piano, F., Gunsalus, K.C.,
730 and Selbach, M. (2016). *In Vivo* Interaction Proteomics in *Caenorhabditis elegans*
731 Embryos Provides New Insights into P Granule Dynamics. Mol. Cell. Proteomics *15*,
732 1642–1657.

733 Chuma, S., Hosokawa, M., Kitamura, K., Kasai, S., Fujioka, M., Hiyoshi, M., Takamune,
734 K., Noce, T., and Nakatsuji, N. (2006). Tdrd1/Mtr-1, a tudor-related gene, is essential for
735 male germ-cell differentiation and nuage/germinal granule formation in mice. Proc. Natl.
736 Acad. Sci. *103*, 15894–15899.

737 Counter, C.M., Avilion, A.A., LeFeuvre, C.E., Stewart, N.G., Greider, C.W., Harley, C.B.,
738 and Bacchetti, S. (1992). Telomere shortening associated with chromosome instability
739 is arrested in immortal cells which express telomerase activity. EMBO J. *11*, 1921–
740 1929.

741 Das, P.P., Bagijn, M.P., Goldstein, L.D., Woolford, J.R., Lehrbach, N.J., Sapetschnig,
742 A., Buhecha, H.R., Gilchrist, M.J., Howe, K.L., Stark, R., et al. (2008). Piwi and piRNAs
743 act upstream of an endogenous siRNA pathway to suppress Tc3 transposon mobility in
744 the Caenorhabditis elegans germline. Mol. Cell *31*, 79–90.

745 Fagagna, F. d'Adda di, Reaper, P.M., Clay-Farrace, L., Fiegler, H., Carr, P., von
746 Zglinicki, T., Saretzki, G., Carter, N.P., and Jackson, S.P. (2003). A DNA damage
747 checkpoint response in telomere-initiated senescence. Nature *426*, 194–198.

748 Guang, S., Bochner, A.F., Pavelec, D.M., Burkhart, K.B., Harding, S., Lachowiec, J.,
749 and Kennedy, S. (2008). An Argonaute Transports siRNAs from the Cytoplasm to the

750 Nucleus. Science (80-.). *321*, 537–541.

751 Guang, S., Bochner, A.F., Burkhart, K.B., Burton, N., Pavelec, D.M., and Kennedy, S.
752 (2010). Small regulatory RNAs inhibit RNA polymerase II during the elongation phase of
753 transcription. Nature *465*, 1097–1101.

754 Harley, C.B., Futcher, A.B., and Greider, C.W. (1990). Telomeres shorten during ageing
755 of human fibroblasts. Nature *345*, 458–460.

756 Heestand, B., Simon, M., Frenk, S., Titov, D., and Ahmed, S. (2018). Transgenerational
757 Sterility of Piwi Mutants Represents a Dynamic Form of Adult Reproductive Diapause.
758 Cell Rep. *23*, 156–171.

759 Herbig, U., Jobling, W.A., Chen, B.P.C., Chen, D.J., and Sedivy, J.M. (2004). Telomere
760 shortening triggers senescence of human cells through a pathway involving ATM, p53,
761 and p21(CIP1), but not p16(INK4a). Mol. Cell *14*, 501–513.

762 Juliano, C., Wang, J., and Lin, H. (2011). Uniting Germline and Stem Cells: The
763 Function of Piwi Proteins and the piRNA Pathway in Diverse Organisms. Annu. Rev.
764 Genet. *45*, 447–469.

765 Karlseder, J., Broccoli, D., Dai, Y., Hardy, S., and de Lange, T. (1999). p53- and ATM-
766 dependent apoptosis induced by telomeres lacking TRF2. Science *283*, 1321–1325.

767 Käser-Pébernard, S., Müller, F., and Wicky, C. (2014). LET-418/Mi2 and SPR-5/LSD1
768 cooperatively prevent somatic reprogramming of C. elegans germline stem cells. Stem
769 Cell Reports *2*, 547–559.

770 Katz, D.J., Edwards, T.M., Reinke, V., and Kelly, W.G. (2009). A C. elegans LSD1
771 demethylase contributes to germline immortality by reprogramming epigenetic memory.

772 Cell *137*, 308–320.

773 Kawasaki, I., Shim, Y.-H., Kirchner, J., Kaminker, J., Wood, W.B., and Strome, S.
774 (1998). PGL-1, a Predicted RNA-Binding Component of Germ Granules, Is Essential for
775 Fertility in C. elegans. Cell *94*, 635–645.

776 Kelleher, E.S. (2016). Reexamining the P-Element Invasion of Drosophila melanogaster
777 Through the Lens of piRNA Silencing. Genetics *203*, 1513–1531.

778 Ketting, R.F., Haverkamp, T.H., van Luenen, H.G., and Plasterk, R.H. (1999). Mut-7 of
779 C. elegans, required for transposon silencing and RNA interference, is a homolog of
780 Werner syndrome helicase and RNaseD. Cell *99*, 133–141.

781 Kidwell, M.G., Kidwell, J.F., and Sved, J.A. (1977). Hybrid Dysgenesis in DROSOPHILA
782 MELANOGASTER: A Syndrome of Aberrant Traits Including Mutation, Sterility and
783 Male Recombination. Genetics *86*, 813–833.

784 Kim, D., Pertea, G., Trapnell, C., Pimentel, H., Kelley, R., and Salzberg, S.L. (2013).
785 TopHat2: accurate alignment of transcriptomes in the presence of insertions, deletions
786 and gene fusions. Genome Biol. *14*, R36.

787 Kim, S.T., Lim, D.S., Canman, C.E., and Kastan, M.B. (1999). Substrate specificities
788 and identification of putative substrates of ATM kinase family members. J. Biol. Chem.
789 *274*, 37538–37543.

790 Knutson, A.K., Egelhofer, T., Rechtsteiner, A., and Strome, S. (2017). Germ Granules
791 Prevent Accumulation of Somatic Transcripts in the Adult Caenorhabditis elegans
792 Germline. Genetics.

793 Krishnamurthy, J., Torrice, C., Ramsey, M.R., Kovalev, G.I., Al-Regaiey, K., Su, L., and

794 Sharpless, N.E. (2004). Ink4a/Arf expression is a biomarker of aging. J. Clin. Invest.
795 *114*, 1299–1307.

796 Krishnamurthy, J., Ramsey, M.R., Ligon, K.L., Torrice, C., Koh, A., Bonner-Weir, S., and
797 Sharpless, N.E. (2006). p16INK4a induces an age-dependent decline in islet
798 regenerative potential. Nature *443*, 453–457.

799 Langmead, B., Trapnell, C., Pop, M., and Salzberg, S.L. (2009). Ultrafast and memory-
800 efficient alignment of short DNA sequences to the human genome. Genome Biol. *10*,
801 R25.

802 Liao, Y., Smyth, G.K., and Shi, W. (2014). featureCounts: an efficient general purpose
803 program for assigning sequence reads to genomic features. Bioinformatics *30*, 923–
804 930.

805 Lowden, M.R., Meier, B., Lee, T.W.S., Hall, J., and Ahmed, S. (2008). End joining at
806 Caenorhabditis elegans telomeres. Genetics *180*, 741–754.

807 Luteijn, M.J., and Ketting, R.F. (2013). PIWI-interacting RNAs: from generation to
808 transgenerational epigenetics. Nat. Rev. Genet. *14*, 523–534.

809 McMurchy, A.N., Stempor, P., Gaarenstroom, T., Wysolmerski, B., Dong, Y.,
810 Aussianikava, D., Appert, A., Huang, N., Kolasinska-Zwierz, P., Sapetschnig, A., et al.
811 (2017). A team of heterochromatin factors collaborates with small RNA pathways to
812 combat repetitive elements and germline stress. Elife *6*.

813 Meier, B., Clejan, I., Liu, Y., Lowden, M., Gartner, A., Hodgkin, J., and Ahmed, S.
814 (2006). trt-1 is the Caenorhabditis elegans catalytic subunit of telomerase. PLoS Genet.
815 *2*, 187–197.

816 Min, H., Shim, Y.-H., and Kawasaki, I. (2016). Loss of PGL-1 and PGL-3, members of a
817 family of constitutive germ-granule components, promotes germline apoptosis in C.
818 elegans. J. Cell Sci. *129*, 341–353.

819 Nakamura, T.M., Cooper, J.P., and Cech, T.R. (1998). Two modes of survival of fission
820 yeast without telomerase. Science *282*, 493–496.

821 Ni, J.Z., Kalinava, N., Chen, E., Huang, A., Trinh, T., and Gu, S.G. (2016). A
822 transgenerational role of the germline nuclear RNAi pathway in repressing heat stress-
823 induced transcriptional activation in C. elegans. Epigenetics and Chromatin *9*, 1–15.

824 Padeken, J., Zeller, P., Towbin, B., Katic, I., Kalck, V., Methot, S.P., and Gasser, S.M.
825 (2019). Synergistic lethality between BRCA1 and H3K9me2 loss reflects satellite
826 derepression. Genes Dev. 1–16.

827 Padilla, P.A., and Ladage, M.L. (2012). Suspended animation, diapause and
828 quiescence. Cell Cycle *11*, 1672–1679.

829 Phillips, C.M., Montgomery, T.A., Breen, P.C., and Ruvkun, G. (2012). MUT-16
830 promotes formation of perinuclear mutator foci required for RNA silencing in the C.
831 elegans germline. Genes Dev. *26*, 1433–1444.

832 Phillips, C.M., Brown, K.C., Montgomery, B.E., Ruvkun, G., and Montgomery, T.A.
833 (2015). piRNAs and piRNA-Dependent siRNAs Protect Conserved and Essential
834 C. elegans Genes from Misrouting into the RNAi Pathway. Dev. Cell *34*, 457–465.

835 R Core Team (2013). R: A language and environment for statistical computing. R
836 Found. Stat. Comput.

837 Robert, V.J., Mercier, M.G., Bedet, C., Janczarski, S., Merlet, J., Garvis, S., Ciosk, R.,

838 and Palladino, F. (2014). The SET-2/SET1 Histone H3K4 Methyltransferase Maintains
839 Pluripotency in the Caenorhabditis elegans Germline.

840 Sakaguchi, A., Sarkies, P., Simon, M., Doebley, A.-L., Goldstein, L.D., Hedges, A.,
841 Ikegami, K., Alvares, S.M., Yang, L., LaRocque, J.R., et al. (2014). Caenorhabditis
842 elegans RSD-2 and RSD-6 promote germ cell immortality by maintaining small
843 interfering RNA populations. Proc. Natl. Acad. Sci. U. S. A. *111*, E4323-31.

844 Sharpless, N.E., and DePinho, R.A. (2007). How stem cells age and why this makes us
845 grow old. Nat. Rev. Mol. Cell Biol. *8*, 703–713.

846 Shay, J.W., and Wright, W.E. (2000). Hayflick, his limit, and cellular ageing. Nat. Rev.
847 Mol. Cell Biol. *1*, 72–76.

848 Shay, J.W., and Wright, W.E. (2005). Senescence and immortalization: role of
849 telomeres and telomerase. Carcinogenesis *26*, 867–874.

850 Simon, M., Sarkies, P., Ikegami, K., Doebley, A.L., Goldstein, L.D., Mitchell, J.,
851 Sakaguchi, A., Miska, E.A., and Ahmed, S. (2014a). Reduced Insulin/IGF-1 Signaling
852 Restores Germ Cell Immortality to Caenorhabditis elegans Piwi Mutants. Cell Rep. *7*,
853 762–773.

854 Simon, M., Sarkies, P., Ikegami, K., Doebley, A.-L., Goldstein, L.D., Mitchell, J.,
855 Sakaguchi, A., Miska, E.A., and Ahmed, S. (2014b). Reduced Insulin/IGF-1 Signaling
856 Restores Germ Cell Immortality to Caenorhabditis elegans Piwi Mutants. Cell Rep. *7*,
857 762–773.

858 Siomi, M.C., Sato, K., Pezic, D., and Aravin, A.A. (2011). PIWI-interacting small RNAs:
859 the vanguard of genome defence. Nat. Rev. Mol. Cell Biol. *12*, 246–258.

860 Smelick, C., and Ahmed, S. (2005a). Achieving immortality in the C. elegans germline.
861 Ageing Res. Rev. *4*, 67–82.

862 Smelick, C., and Ahmed, S. (2005b). Achieving immortality in the C. elegans germline.
863 Ageing Res. Rev. *4*, 67–82.

864 Spracklin, G., Fields, B., Wan, G., Vijayendran, D., Wallig, A., Shukla, A., and Kennedy,
865 S. (2017). Identification and Characterization of Caenorhabditis elegans RNAi
866 Inheritance Machinery. Genetics.

867 Srivastav, S.P., and Kelleher, E.S. (2017). Paternal Induction of Hybrid Dysgenesis in
868 *Drosophila melanogaster* Is Weakly Correlated with Both *P* -Element and *hobo* Element
869 Dosage. G3: Genes|Genomes|Genetics *7*, 1487–1497.

870 Strome, S., and Wood, W.B. (1982). Immunofluorescence visualization of germ-line-
871 specific cytoplasmic granules in embryos, larvae, and adults of Caenorhabditis elegans.
872 Proc. Natl. Acad. Sci. U. S. A. *79*, 1558–1562.

873 Sung, M., Kawasaki, I., and Shim, Y.-H. (2017). Depletion of *cdc-25.3* , a
874 *Caenorhabditis elegans* orthologue of *cdc25* , increases physiological germline
875 apoptosis. FEBS Lett. *591*, 2131–2146.

876 Tatar, M., and Yin, C. (2001). Slow aging during insect reproductive diapause: why
877 butterflies, grasshoppers and flies are like worms. Exp. Gerontol. *36*, 723–738.

878 Tchkonia, T., Zhu, Y., van Deursen, J., Campisi, J., and Kirkland, J.L. (2013). Cellular
879 senescence and the senescent secretory phenotype: therapeutic opportunities. J. Clin.
880 Invest. *123*, 966–972.

881 Updike, D., and Strome, S. (2010). P Granule Assembly and Function in Caenorhabditis

882 elegans Germ Cells. J. Androl. *31*, 53–60.

883 Updike, D.L., Hachey, S.J., Kreher, J., and Strome, S. (2011). P granules extend the
884 nuclear pore complex environment in the *C. elegans* germ line. J. Cell Biol. *192*, 939–
885 948.

886 Updike, D.L., Knutson, A.K., Egelhofer, T.A., Campbell, A.C., and Strome, S. (2014).
887 Germ-Granule Components Prevent Somatic Development in the C. elegans Germline.
888 Curr. Biol. *24*, 970–975.

889 Vermezovic, J., Stergiou, L., Hengartner, M.O., and d'Adda di Fagagna, F. (2012).
890 Differential regulation of DNA damage response activation between somatic and
891 germline cells in Caenorhabditis elegans. Cell Death Differ. *19*, 1847–1855.

892 Zeller, P., Padeken, J., van Schendel, R., Kalck, V., Tijsterman, M., and Gasser, S.M.
893 (2016). Histone H3K9 methylation is dispensable for Caenorhabditis elegans
894 development but suppresses RNA:DNA hybrid-associated repeat instability. Nat. Genet.
895 *48*, 1385–1395.

896 Zheng, K., and Wang, P.J. (2012). Blockade of Pachytene piRNA Biogenesis Reveals a
897 Novel Requirement for Maintaining Post-Meiotic Germline Genome Integrity. PLoS
898 Genet. *8*, e1003038.

899

900

901 **Table 1**

Percent of germlines showing P granule abnormalities

	fertile	sterile
	20˚C	
wt (n=12)	0.00%	NA
prg-1(n4357) (n=16)	36.36%	100.00%
prg-1(tm872) (n=21)	87.50%	92.31%
nrde-4(gg131) (n=13)	50.00%	90.91%
nrde-1(yp4) (n=13)	20.00%	87.50%
	25˚C	
wt (n=35)	0.00%	NA
mut-14(pk738) (n=15)	NA	85%
rsd-6(yp11) (n=32)	0.00%	40.00%
nrde-2(gg95) (n=25)	0.00%	100.00%
rbr-2(tm1231) (n=32)	0.00%	100.00%
hrde-1(tm1200) (n=31)	0.00%	100.00%

902

903 **Table 1: Quantification of P granule defects in the germline.**

904 Sterile Piwi pathway genome silencing mutants were stained with P granule antibody.
905 Germlines arms were semi-qualitatively scored for P granules. If 20% or more of the the
906 germline arm exhibited P granules abnormalities (complete or partial loss of P granules)
907 germlines were scored as abnormal.

908

909

910

911 **Supplemental Information**

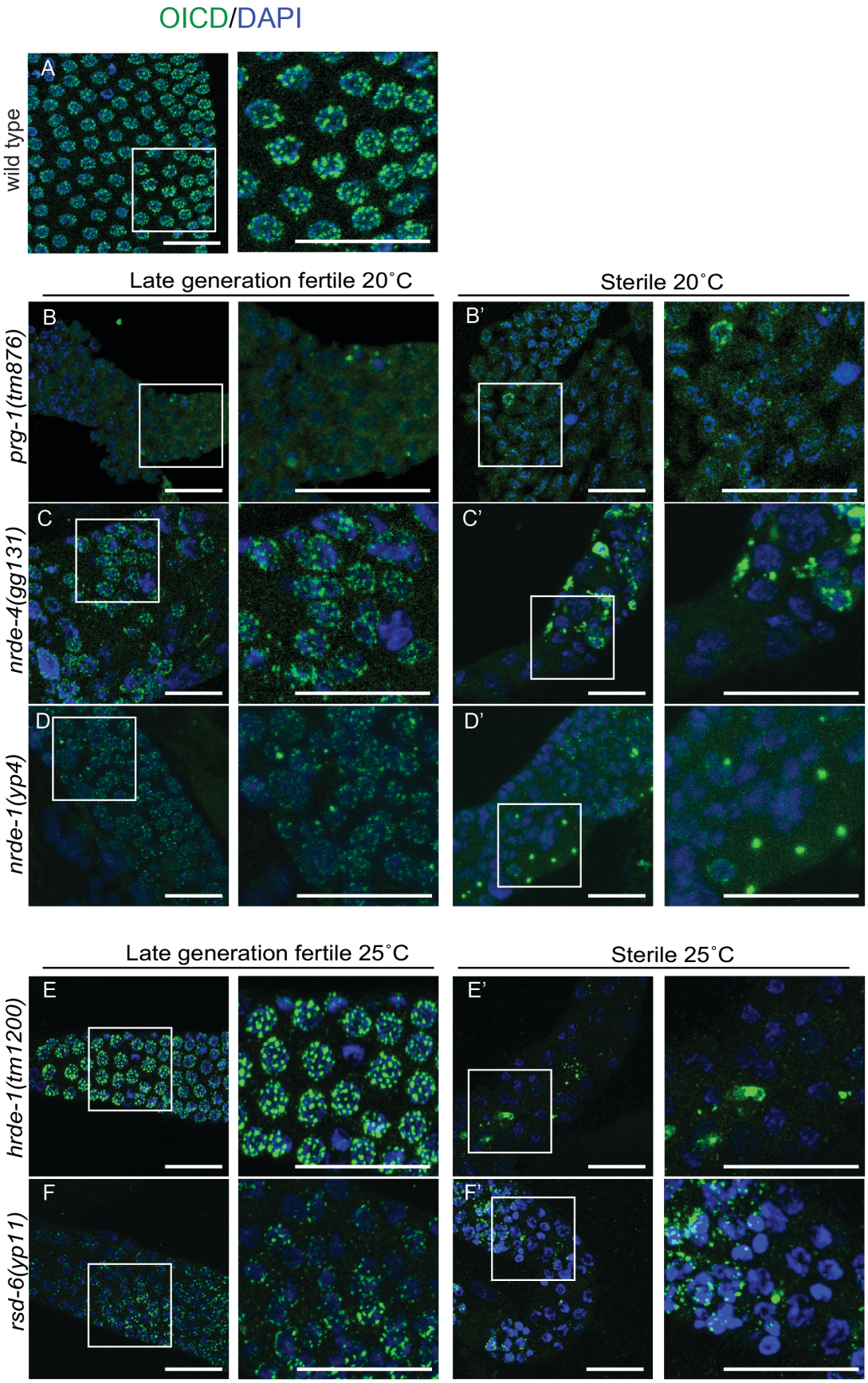
OICD/DAPI
A
wild type
Late generation fertile 20˚C
Sterile 20˚C
B
B'
prg-1(tm876)
C
C'
nrde-4(gg131)
D
D'
nrde-1(yp4)
Late generation fertile 25˚C
Sterile 25˚C
E
E'
hrde-1(tm1200)
F
F'
rsd-6(yp11)

912

913 **Fig. S1. Related to Figure 2. P granule defects in *prg-1, nrde- 4, hrde-1 and nrde-1*.**
914 Germlines of sterile Day 2-3 adult animals were stained using the OIC1D4 antibody
915 against P granules (green) and DAPI (blue). (A) Control animals contain uniform puncta
916 of P granule staining surrounding each nuclei. (B-F) Late generation fertile *prg-*
917 *1(tm876), nrde-4(gg131), nrde-1(yp4)*, *hrde-1(tm1200)* and *rsd-6(yp11)* and animals
918 displayed P granule staining similar to wild type except for *prg-1(tm876).* (B'-F') Sterile
919 *prg-1(tm876), nrde-4(gg131), nrde-1(yp4)*, *hrde-1(tm1200)* and *rsd-6(yp11)* with P
920 granule abnormalities.

921

	Total Worms Scored	% Fertile	% Sterile
pgl-1 G1 at 25°C	91	22%	78%
pgl-1 G2 at 25°C	71	0%	100%

922

923 **Table S1: Related to Figure 3. Fertility of *pgl-1* mutants at 25°C.** 20°C P0 *pgl-1*
924 mutants were shifted to 25°C and fertility was measured for the G1 generation. Fertile
925 G1 worms were cloned and the fertility of the G2 generation was measured.

926

927

gene	***prg-1***	***nrde-1***	***nrde-4***
C06B3.7	4.331128036	1.732445354	2.669978253
dhs-26	3.88587979	3.752818032	1.793937273
bath-45	3.604851731	5.5002102	2.319444032
fbxb-97	3.555301139	3.002992933	3.278539846
irg-2	3.519633623	2.605415087	2.189754742
pud-4	3.226292885	2.956152303	4.407697185
pud-3	3.097392415	3.143142026	4.328678969
R09E10.2	2.745900789	5.100997358	4.251177196
Y53F4B.5	2.636725232	5.821227047	4.162462556
K08D12.6	2.631068263	2.955437046	0.277803871
R03H10.6	2.469258519	4.82098578	3.295830487
Y58A7A.5	2.397260966	1.795895	2.143861408
pud-1.1	2.299685196	2.556376909	3.17781014
T22B7.7	2.276777478	3.01143186	2.207919501
fbxa-224	2.248998131	4.226992478	1.979961678
swt-6	2.144598564	3.153313277	0.277029378
pud-2.1	2.119890425	2.781615959	2.880747229
pud-2.2	2.094123631	2.779337879	2.796566876
pud-1.2	2.080250623	2.559790088	3.000944771
catp-3	2.014970724	2.436698711	2.674464594

928

929 **Table S2: Related to Figure 4. Genes upregulated in late-generation *prg-1* mutants**
930 **and in sterile *nrde-1* and *nrde-4* mutant L4 larvae.**
931